Conformation-specific infrared and ultraviolet spectroscopy of tyrosine-based protonated dipeptides

Jaime A. Stearns, Monia Guidi, Oleg V. Boyarkin, and Thomas R. Rizzo

Citation: J. Chem. Phys. **127**, 154322 (2007); doi: 10.1063/1.2798111
View online: http://dx.doi.org/10.1063/1.2798111
View Table of Contents: http://jcp.aip.org/resource/1/JCPSA6/v127/i15
Published by the AIP Publishing LLC.

Conformation-specific infrared and ultraviolet spectroscopy of tyrosine-based protonated dipeptides

Jaime A. Stearns,[a] Monia Guidi, Oleg V. Boyarkin, and Thomas R. Rizzo
Laboratoire de Chimie Physique Moléculaire, Ecole Polytechnique Fédérale de Lausanne, EPFL SB ISIC LCPM, Station 6, CH-1015 Lausanne, Switzerland

(Received 24 August 2007; accepted 19 September 2007; published online 19 October 2007)

We present the spectroscopy and photofragmentation dynamics of two isomeric protonated dipeptides, H^+AlaTyr and H^+TyrAla, in a cold ion trap. By a combination of infrared-ultraviolet double resonance experiments and density functional theory calculations, we establish the conformations present at low temperature. Interaction of the charge at the N-terminus with the carbonyl group and the tyrosine π-cloud seems to be critical in stabilizing the low-energy conformations. H^+AlaTyr has the flexibility to allow a stronger interaction between the charge and the aromatic ring than in H^+TyrAla, and this interaction may be responsible for many of the differences we observe in the former: a significant redshift in the ultraviolet spectrum, a much larger photofragmentation yield, fewer stable conformations, and the absence of fragmentation in excited electronic states. © *2007 American Institute of Physics*. [DOI: 10.1063/1.2798111]

I. INTRODUCTION

One of the primary goals of spectroscopic studies of small, gas-phase peptides is to understand the driving forces for the conformational preferences in proteins, particularly the formation of secondary structural features such as α or γ turns, or β sheets, often using the aromatic amino acids as conformational probes. Beginning with the first electronic spectrum of jet-cooled tryptophan,[1] which contains features from six different stable conformers, the field has blossomed as infrared-ultraviolet (IR-UV) double resonance techniques combined with quantum chemical calculations often lead to unambiguous assignment of the secondary structure. Most of these studies are carried out in supersonic expansions using either sample heating or laser desorption to bring neutral peptides into the gas phase together with detection schemes based on fluorescence or ionization.[2–6] Most peptides are closed-shell ions in solution, however, and stabilization of the charge by interaction with various functional groups provides one of the driving forces for peptide structure. We have recently developed a method to investigate the structure of protonated biomolecules, using electrospray ionization to transfer them into the gas phase before cooling them in a low-temperature ion trap and interrogating them by photofragment spectroscopy.[7–9] IR-UV double resonance spectroscopy of the protonated aromatic amino acids tyrosine and phenylalanine, together with density functional theory calculations, allowed us to establish the stable conformations of these species present in the gas phase at low temperature.[9] All detected conformations of both molecules exhibit strong interactions between the ammonium group and both the aromatic π cloud and the carbonyl oxygen and can be divided according to the orientation of the carboxylic acid group with respect to the ring, either in an *anti* or *gauche* arrangement. In the case of protonated tyrosine, the different classes of conformations exhibit different photodissociation dynamics.

Here we use the foundation of our previous work[7,9] on $TyrH^+$ to study the spectroscopy and photofragmentation dynamics of two isomeric N-terminal-protonated dipeptides, H^+AlaTyr and H^+TyrAla. Cohen *et al.*[10] measured ultraviolet spectra of both dipeptides in their neutral form in a supersonic expansion, finding electronic spectra similar to that of neutral tyrosine. The number of conformers of neutral AlaTyr and TyrAla and their structures were not established beyond classification into *anti* and *gauche* forms,[10] although the gas-phase structures of other comparable Phe- and Trp-containing natural and model dipeptides have been more fully determined.[2–4,11–14] Peptide structures are characterized by the hydrogen bonding interactions among the backbone amide groups, with the simplest being the C_5 interaction—a weak hydrogen bond between an amide NH and the carbonyl oxygen on the same amino acid. A stronger interaction occurs when the amide NH hydrogen bonds to the carbonyl oxygen on the previous amino acid, forming a seven-membered ring (C_7). The C_5 and C_7 interactions account for the structure observed in neutral dipeptides and dipeptide mimics, including those based on Phe (Ref. 4 and 11–14) and Trp.[2,3] In the protonated dipeptides, charge interactions will provide additional driving forces that may alter the conformational landscape and the photofragmentation dynamics. To more fully understand the role of charge, we use a combination of infrared-ultraviolet double resonance spectroscopy and density functional theory calculations to investigate the preferred structural motifs of gas-phase H^+AlaTyr and H^+TyrAla.

II. EXPERIMENTAL AND COMPUTATIONAL METHODS

The experimental apparatus used in these experiments has been described previously.[7,9] Protonated AlaTyr and TyrAla (Bachem, Inc.) are generated by a nanoelectrospray source from a typical solution concentration of 2×10^{-4}M in

[a]Electronic mail: jaime.stearns@epfl.ch

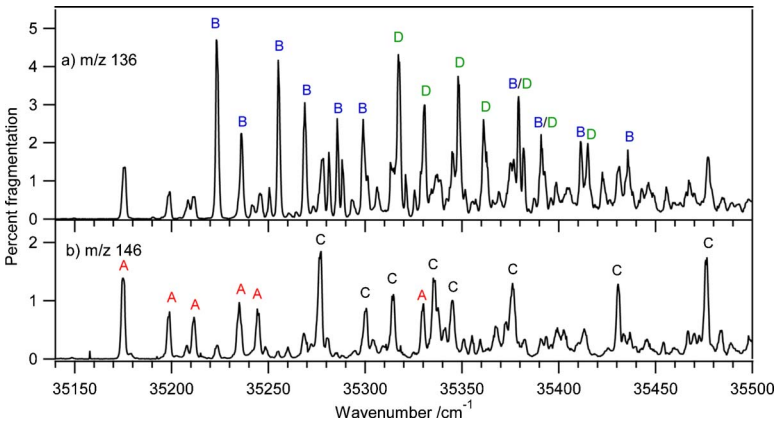

FIG. 1. (Color online) Ultraviolet photofragmentation spectra of H^+TyrAla recorded by fragmentation into (a) mass channel 136 and (b) mass channel 146. The transitions are labeled by conformation, as determined by infrared-ultraviolet double resonance spectroscopy. The same transitions are present with different intensities in both spectra, but are only labeled in one for clarity. The mass of the parent molecule is 253 amu.

50:50 methanol:water with 0.2% acetic acid and collected in a hexapole ion trap. After ~41 ms, the ions are released from the hexapole, passed through a quadrupole mass filter, and guided into a 22-pole ion trap that is maintained at 6 K, where they are cooled by collisions with helium. After being interrogated by the lasers, the cold ions are released from the trap and passed through a second quadrupole mass filter to detect photoinduced fragments.

We measure three kinds of spectra in these experiments. In the first type, we record ultraviolet photofragmentation excitation spectra by monitoring the fragment at a particular m/z as a function of the UV laser frequency. This provides an electronic spectrum of the cold parent molecules that contains features from the stable conformations populated at the temperature of our cold trap. In a second type of experiment, we measure fragmentation mass spectra by selecting an ultraviolet transition and tuning the second quadrupole across the fragment mass range, providing information on the photofragmentation efficiency into various channels. In a third type of experiment, we record conformation-specific infrared spectra. In this case, we set the UV laser on a feature of the electronic spectrum associated with a particular conformation and introduce an infrared laser ~100 ns earlier. When the IR laser is resonant with a vibrational transition in the ion, population is removed from the ground state of that conformation. If the IR and UV lasers are probing the same conformation and if the vibrationally excited molecules absorb the UV less efficiently, the reduced ground state population results in a depletion in the UV photofragment signal. We record the spectrum by monitoring the difference in the photofragment signal with the IR laser on or off as a function of the IR frequency. We use the IR spectra as a fingerprint to associate each peak in the UV spectra with a particular conformer. All spectra are normalized for parent ion signal and for laser pulse energy, typical values of which are 5 mJ in the UV and 10 mJ in the IR.

We assumed the dipeptides to be protonated at the N terminus and used the conformational search algorithm in MACROMODEL (Ref. 15) with the AMBER force field[16] to find the low-energy conformations. We then carried out reoptimization and harmonic frequency analysis on the lowest-energy structures from this search using density functional theory in GAUSSIAN 03 (Ref. 17) at the B3LYP/6-31++G^{**} level. We chose a scale factor of 0.954 for all harmonic frequencies, which gives good agreement with the measured frequencies in our previous work on the protonated aromatic amino acids.[9] The relative energies we report here for the dipeptides include zero-point energy corrections based on the unscaled harmonic frequencies.

III. RESULTS AND DISCUSSION

A. H^+TyrAla

Figure 1 shows the ultraviolet photofragmentation spectrum of H^+TyrAla (m/z 253), recorded via the two primary fragmentation channels, m/z 136 [Fig. 1(a)] and m/z 146 [Fig. 1(b)]. The fragment with m/z 136 is the protonated imine $NH_2^+=CH-CH_2-Ph-OH$, which results from cleavage of the $C_\alpha-C_{amide}$ bond, part of a common reaction mechanism in collision-induced dissociation (CID) of dipeptides known as the a_1-y_1 pathway.[18] The fragment at m/z 146 results from loss of the tyrosine side chain radical, a reaction that we attributed to dissociation on an excited electronic state in $TyrH^+$.[9] The lowest energy transition, which occurs at 35 174.8 cm^{-1}, has approximately the same intensity in each spectrum, corresponding to fragmentation of ~1% of the parent ion population. The largest peak in the spectrum of Fig. 1(a), which occurs at 35 223.2 cm^{-1}, shows significantly different behavior, giving rise to a fragmentation signal nearly 5% of the parent when measured at the m/z 136 signal, but only 0.2% when measured at m/z 146. The different fragmentation patterns of these two transitions are confirmed by their fragmentation mass spectra, shown in Fig. 2. This strongly suggests that the two transitions are the band origins of different conformers, which we label A and B. Although the conformer A origin appears less intense than that of conformer B in Fig. 1, the total fragmentation yield is similar for the two conformers once we take into account the different fragmentation patterns. The difference in energy between these two band origins is 48 cm^{-1}, which is similar to the 30 cm^{-1} splitting observed between those of the *anti* and *gauche* conformers of $TyrH^+$.[9]

Figure 3 shows the NH stretch region of the IR spectra recorded with the UV laser set to the presumed electronic band origins of conformers A and B. Each spectrum exhibits two NH stretch peaks in the region between 3350 and 3400 cm^{-1}, which are assigned to free NH stretches. The two peaks are split by 22 cm^{-1} in conformer A and 14 cm^{-1} in

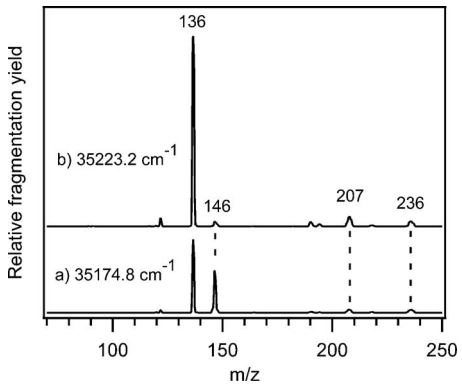

FIG. 2. Fragmentation mass spectra of H^+TyrAla recorded at (a) 35 174.8 cm^{-1} and (b) 35 223.2 cm^{-1}, with the major fragment peaks labeled. The parent mass is 253 amu.

conformer B, and the set of peaks in conformer B is blue-shifted from that of conformer A by about 15 cm^{-1}. The broad peaks in the lower frequency region of 3100–3200 cm^{-1} are assigned to the ammonium NH stretches involved in hydrogen bonds,[9] and again A and B show differences in this region. These spectra confirm that A and B are different conformers.

The lowest-energy calculated structures of H^+TyrAla are all characterized by three hydrogen bonding interactions: an $NH\cdots\pi$ hydrogen bond between the ammonium group and the aromatic ring and $NH\cdots O{=}C$ C_5 interactions on both the ammonium group and the neutral amide NH group (Fig. 4, top row). We designate these four structures as belonging to conformer family I. Within this family, there are two possible rotations about the tyrosinyl C_α–C_β bond (the χ_1 dihedral angle) such that the COOH group is *anti* or *gauche* to the ring and two orientations of the phenolic oxygen lone pair of electrons with respect to the ammonium group (*syn* or *anti*). The orientation of the phenolic oxygen has little effect on the conformer energy (0.1 kJ/mol), while the *anti* backbone conformations are stabilized 4 kJ/mol relative to the *gauche* conformers.

The other calculated conformers can be similarly sorted into families of hydrogen bonding patterns (Fig. 4, families

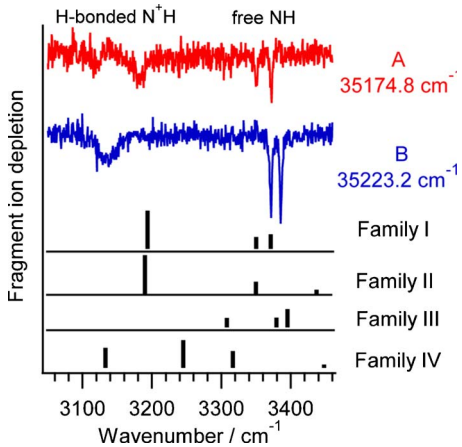

FIG. 3. (Color online) Infrared spectra of the NH stretch region of H^+TyrAla, recorded with the UV laser set to 35 174.8 and 35 223.2 cm^{-1}, together with calculated spectra of four conformational families.

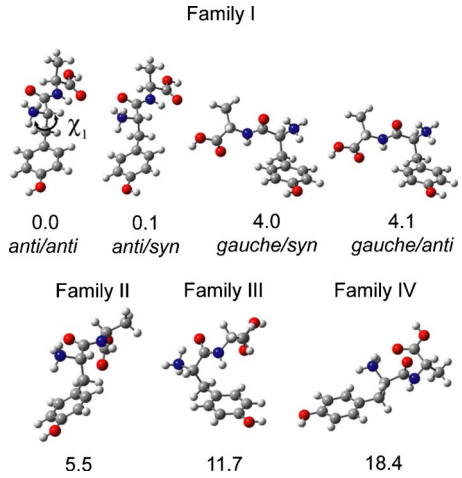

FIG. 4. (Color online) Structures and zero-point-corrected energies in kJ/mol of H^+TyrAla calculated at the B3LYP/6-31++G^{**} level of theory. The four lowest energy structures (family I) are all characterized by a C_5 interaction and a π-hydrogen bond of the ammonium group and a C_5 interaction of the amide NH. The structures are named according to the orientation of the COOH with respect to the ring (*anti* or *gauche*) and the location of the phenol oxygen lone pair with respect to the ammonium group (*anti* or *syn*). Three representative structures of higher energy families (II–IV) are also shown.

II–IV). The ammonium group in family II has the C_5 interaction and π-hydrogen bond, but the amide NH is free from any H bonding. The carboxylic acid C=O points into the tyrosine C_β hydrogens, providing a stabilizing interaction indicated by the calculated carbonyl stretch frequency, which is 40 cm^{-1} lower than that of a free carbonyl and 10 cm^{-1} higher than that of a carbonyl in a C_5 interaction. The lowest-energy member of this family is 5.5 kJ/mol above the global minimum. The next family (III), 11.7 kJ/mol higher in energy, is characterized by the absence of an $NH_3\cdots\pi$ hydrogen bond, with an amide $NH\cdots\pi$ hydrogen bond in its place. Finally, there are structures of 18.4 kJ/mol and higher which do not exhibit extended backbone structures but which form eight-membered hydrogen bonded rings (family IV). This C_8 ring is formed by the hydrogen bond between the NH group of one amino acid and the carbonyl of the next amino acid, whereas the C_7 ring observed[2,4] in the neutral peptides connects an amide NH with the carbonyl of the *previous* amino acid. The C_7 ring is thus found in dipeptide mimics that are capped at both ends or in larger molecules (e.g., tripeptides), but not in uncapped dipeptides.

Figure 3 shows the calculated infrared spectra of the lowest-energy conformer of each family in comparison with the experimental spectra of conformers A and B. It is clear that family I accounts best for the experimental spectra. We can assign conformers A and B more precisely by comparison with the calculated spectra of the four conformers in family I, as shown in Fig. 5. The 15 cm^{-1} difference between the free NH stretches of A and B is reflected in the calculated spectra as the difference between the *anti* and *gauche* backbone orientations, allowing us to assign conformer A to an *anti* structure and conformer B to the slightly higher energy *gauche* conformer.

Based on the calculations and our previous experience with $TyrH^+$,[9] we expect to find two additional conformers

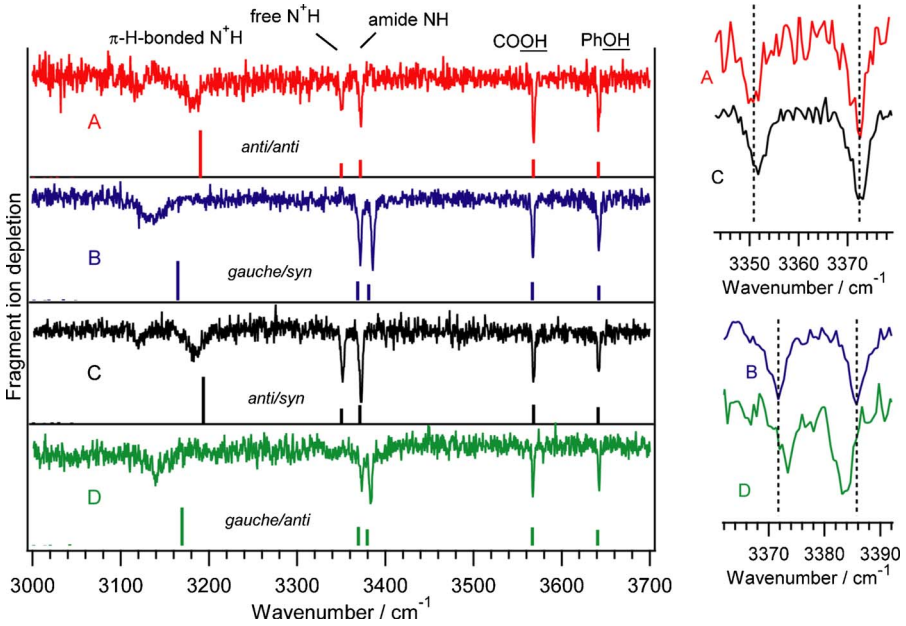

FIG. 5. (Color online) Infrared spectra of the four band origins of H^+TyrAla, located at 35 174.8 cm^{-1} (A), 35 223.2 cm^{-1} (B), 35 277.2 cm^{-1} (C), and 35 317.1 cm^{-1} (D). The calculated stick spectra are shown for the four conformers of family I, showing conformers A and C to be *anti* conformers and B and D to be *gauche* conformers. The right panel shows the free NH stretch region expanded. Conformer D is distinguished from conformer B by the smaller splitting of the free NH stretches, while the free ammonium NH stretch of conformer A is slightly but reproducibly lower in frequency than that of conformer C. The dashed lines are through the center of the peaks of conformers A and B to highlight the differences. The assignment of the absolute orientation of the phenolic OH group is uncertain, given the small differences in the spectra.

with the same structures as A and B but the opposite phenol OH orientation. We found the band origin of a third conformer (C), which is the largest peak in Fig. 1(b), at 35 277.2 cm^{-1}, or 102 cm^{-1} above the band origin of conformer A. The IR spectrum of C (Fig. 5) differs from that of A primarily in the free ammonium NH stretch, which appears reproducibly one wave number lower in A than in C. The calculations predict a slightly larger splitting in the free NH peaks for the *anti/anti* conformer (22 cm^{-1}) as compared to the *anti/syn* conformer (21 cm^{-1}), but this difference is too small to allow a definitive assignment. The origin of the fourth conformer (D) is located at 35 317.1 cm^{-1}, 94 cm^{-1} above the B origin. Again the IR spectra of these two conformers differ in the free NH stretch region, with a 14 cm^{-1} splitting for B and a 10 cm^{-1} splitting for D. The splittings are calculated to be 12 cm^{-1} in the *gauche/syn* conformer and 10 cm^{-1} in the *gauche/anti* conformer.

One NH stretch does not appear in Fig. 5—that of the ammonium NH which is in a C_5 arrangement with the amide carbonyl. In $TyrH^+$ this vibration is coupled to the π-hydrogen-bonded NH stretch, appearing as symmetric and antisymmetric combinations of the two vibrations.[9] In H^+TyrAla, however, the C_5 interaction is much stronger, evidenced by the decoupling of the NH···O=C and NH···π stretches. Our calculations predict the local mode π-hydrogen-bonded NH stretch to be between 3100 and 3200 cm^{-1} and the C_5 NH stretch to be around 2950 cm^{-1} in the *anti* conformers and 2800 cm^{-1} in the *gauche* conformers. The physical origin of the stronger C_5 interaction is the better alignment of the NH and C=O groups as measured by the dihedral angle between them, which is calculated to be 10° in $TyrH^+$ but just 3° (7°) in the *gauche* (*anti*) conformers of H^+TyrAla. We scanned the region below 3000 cm^{-1} using all four band origins but saw no depletion. We speculate that these vibrational bands are broadened considerably, making them difficult to detect.

The conformers we observe in H^+TyrAla are analogous to those observed[9] in $TyrH^+$ and both systems exhibit excited-state fragmentation involving loss of the side chain radical. The excited-state dissociation was much more prominent in $TyrH^+$, where it accounted for nearly all the products observed, although more so in the *anti* conformers than in the *gauche*. In the H^+TyrAla *anti* conformers, excited-state dissociation accounts for one-third of the photofragments, while in the *gauche* conformers it is at most 2%. The mechanism of excited-state fragmentation is not clear, even in $TyrH^+$, but it likely originates from the coupling between the bright $\pi\pi^*$ state and a dark $\pi\sigma^*$ state that is repulsive along the ammonium N–H stretch coordinates and can lead to loss of hydrogen or the transfer of a proton or hydrogen atom within the molecule.[19,20] Fission of the C_α–C_β bond may occur subsequent to this initial excited-state dissociation or transfer event. Our fragmentation data suggest that the *anti* conformers possess stronger coupling between the $\pi\pi^*$ and $\pi\sigma^*$ states and/or lower barriers to the excited-state dissociation processes.

B. H^+AlaTyr

Figure 6 shows the ultraviolet photofragmentation spectrum of H^+AlaTyr. The electronic band origin, which appears at 34 525.2 cm^{-1}, is shifted 650 cm^{-1} to the red of the lowest energy band origin of H^+TyrAla, indicating a relative stabilization of the excited state. One source of stabilization is the stronger interaction between the NH_3^+ and the π system of the phenol side chain in H^+AlaTyr. Because the charge is

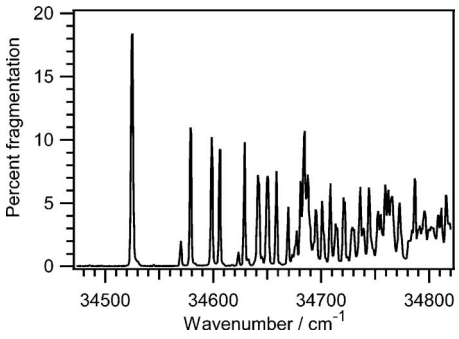

FIG. 6. Ultraviolet photofragmentation spectrum of H^+AlaTyr, recorded using the fragment at m/z 182.

now separated from the aromatic ring by six bonds (as opposed to three in H^+TyrAla), it can get much closer to the π cloud and thus interact more strongly.

The fragmentation yield in Fig. 6 is nearly 20%, considerably higher than that observed for H^+TyrAla or the protonated aromatic amino acids, which was only a few percent.[9] One reason for this apparently higher yield is the fragmentation pattern of H^+AlaTyr, shown in Fig. 7. Most of the fragmentation occurs into a single mass channel, m/z 182, which corresponds to the mass of protonated tyrosine. This fragment results from the a_1-y_1 dissociation pathway, which is commonly observed in the CID of dipeptides.[18] The first three vibronic bands in the UV spectrum all exhibit the same fragmentation mass spectrum as the origin. Unlike H^+TyrAla and the protonated aromatic amino acids,[9] there is no indication of excited-state fragmentation of H^+AlaTyr, which would be evidenced by breakage of the tyrosinyl C_α–C_β bond to give fragments at m/z 107 and/or 146. The proximity of the ammonium group to the aromatic ring in H^+AlaTyr may alter the relationship between the $\pi\pi^*$ and $\pi\sigma^*$ states such that internal conversion dominates.

Our density functional theory calculations predict the existence of several low-energy families of conformations that give rise to unique infrared spectra. The global minimum (Fig. 8, family I) has a strong interaction between the ammonium group and the phenol π cloud in addition to the C_5 interactions of the ammonium and amide NH bonds with the carbonyls. In H^+TyrAla the corresponding conformer was accompanied by a *gauche* structure of similar energy, but in H^+AlaTyr the *gauche* structure has the ammonium group positioned remotely from the ring with the loss of the favorable hydrogen bonding interaction (Fig. 8, family III). Surprisingly, family III is only 1.7 kJ/mol higher in energy than family I, whereas the energy difference for the seemingly more similar *anti* and *gauche* structures of H^+TyrAla is 4 kJ/mol (Fig. 4). Families II–IV are similar in that they all lack the $NH_3\cdots\pi$ interaction but have an amide $NH\cdots\pi$ interaction instead, much like family III of H^+TyrAla. Families II and IV of H^+AlaTyr have the same hydrogen bonding structure, but the COOH group is *gauche* to the ring in family II and *anti* in family IV. Because this gives rise to a difference in the IR spectrum, both structures are considered separately here. Finally, family V exhibits an eight-member hydrogen-bonded ring between the N terminus and C terminus of the dipeptide and is much higher in energy (11.5 kJ/mol), although not as high as the corresponding family IV of H^+TyrAla. The calculated IR spectrum of each of these conformer families is shown in Fig. 9 along with the experimental spectrum recorded with the UV excitation at the H^+AlaTyr origin.

The stick spectrum of family I is the only reasonable match to the experimental spectrum, predicting two bands in

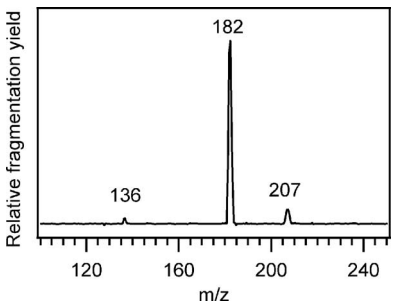

FIG. 7. Fragmentation mass spectrum of H^+AlaTyr, recorded at the electronic origin at 34 525.2 cm^{-1}. The parent ion mass is 253 amu.

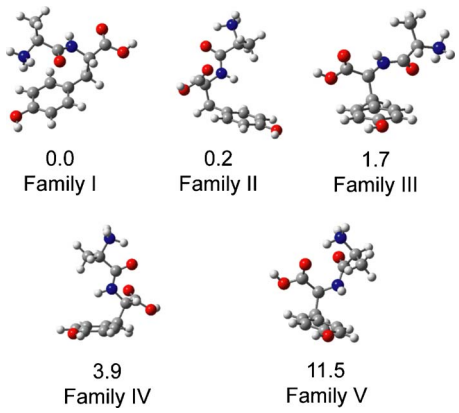

FIG. 8. (Color online) Families of H^+AlaTyr structures calculated using B3LYP/6-31++G^{**}. Energies are given in kJ/mol and are zero-point corrected.

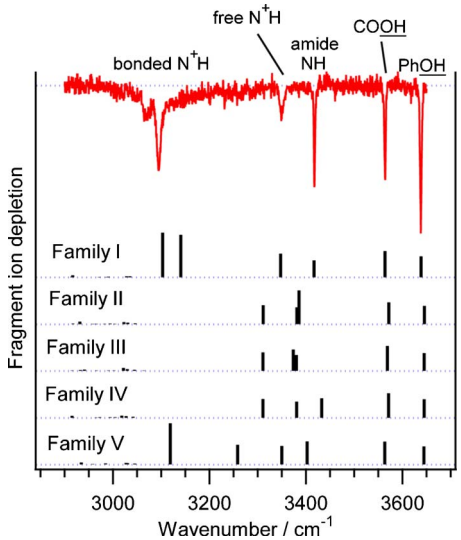

FIG. 9. (Color online) Infrared-ultraviolet depletion spectrum of H^+AlaTyr recorded at the electronic origin at 34 525.2 cm^{-1}, with the peaks assigned by comparison to the calculated spectra of five conformer families.

the 3300–3400 cm^{-1} region arising from the free ammonium NH and amide NH stretches and two strong bands below 3100 cm^{-1} from the symmetric and antisymmetric combinations of the π-hydrogen-bonded and C_5 ammonium NH stretches. This calculated spectrum is not unique, however, as there are three conformers in family I in addition to that shown in Fig. 8, which differ in the orientation of the phenolic OH or COOH groups but have indistinguishable spectra. These rotational isomers are unlikely to exist in our experiment because they are all calculated to be more than 6 kJ/mol higher in energy than the conformer shown in Fig. 8. This energy difference, which is only 0.1 kJ/mol in the corresponding conformers of H^+TyrAla, arises from the fact that the ammonium group resides on one side of the aromatic ring, so a more favorable interaction is achieved when the phenolic lone pair points to that same side.

We used the IR-UV double resonance techniques to search for other conformers, but the IR spectra associated with all the UV peaks we examined were the same. We also performed the complementary hole-burning experiments in which the IR wave number was fixed on a particular transition while the UV frequency was scanned and found that IR transitions at 3095, 3349, and 3418 cm^{-1} deplete every UV peak, indicating that they are associated with a single conformer or with conformers that have the same IR spectrum. The evidence from the IR spectra, together with the relative energetics of the conformers of family I, suggests that there is only a single conformer responsible for the UV spectrum of Fig. 6. The concentration of the population into a single conformer is consistent with the large fragmentation yield relative to the aromatic amino acids and H^+TyrAla, in which the population is spread over several conformers. This high yield is thus a consequence of a single conformer that fragments into a single significant mass channel, in addition to the possibility of an inherently stronger absorption. The presence of a single conformation is somewhat surprising given the low energies of families II–IV, but this is likely a consequence of the level of theory used, and perhaps an overestimation of the energy of family I.

IV. CONCLUSIONS

IR-UV double resonance spectra of the cold, protonated dipeptides H^+TyrAla and H^+AlaTyr reveal hydrogen bonding patterns that allow us to distinguish between calculated families of low-energy structures. The conformations of both dipeptides exhibit an extended backbone motif similar to that observed in the protonated aromatic amino acids,[9] with C_5 and π-hydrogen-bonding interactions stabilizing the charge on the ammonium group. This interaction is weaker in H^+TyrAla because of the smaller number of bonds from the charged ammonium to the phenol ring, allowing the possibility to adopt four stable conformers of the same general family. In H^+AlaTyr, the increased number of bonds between the charge and the aromatic ring allows for a closer contact and hence stronger interaction, seemingly stabilizing a single conformer compared to other possibilities.

These results verify the importance of the charged group in driving the conformational preferences in small peptides. When placed in solution, the interaction between the ammonium and other groups on the molecule will compete with solvation of the charge by water, and the subtle interplay between these forces will determine the solution-phase conformation. This competition can equally be probed in the gas phase by performing spectroscopic studies of hydrated clusters of protonated biomolecules.[8,21] Finally, the strong interaction between the charged N terminus and the aromatic ring facilitated by the flexibility in H^+AlaTyr may play an important role in the photodissociation dynamics, as it is likely to shift the relative positions of $\pi\pi^*$ and $\pi\sigma^*$ states.[20]

ACKNOWLEDGMENTS

We gratefully acknowledge funding for this work provided by the École Polytechnique Fédérale de Lausanne and the Fonds National Suisse through Grant No. 200020-112074.

[1] T. R. Rizzo, Y. D. Park, L. A. Peteanu, and D. H. Levy, J. Chem. Phys. **84**, 2534 (1986).
[2] B. C. Dian, A. Longarte, S. Mercier, D. Evans, D. J. Wales, and T. S. Zwier, J. Chem. Phys. **117**, 10688 (2002).
[3] I. Huenig and K. Kleinermanns, Phys. Chem. Chem. Phys. **6**, 2650 (2004).
[4] W. Chin, F. Piuzzi, I. Dimicoli, and M. Mons, Phys. Chem. Chem. Phys. **8**, 1033 (2006).
[5] M. Gerhards, in *Principles of Mass Spectrometry Applied to Biomolecules*, edited by J. Laskin and C. Lifshitz (Wiley, Hoboken, NJ, 2006), p. 3.
[6] M. S. de Vries and P. Hobza, Annu. Rev. Phys. Chem. **58**, 585 (2007).
[7] O. V. Boyarkin, S. R. Mercier, A. Kamariotis, and T. R. Rizzo, J. Am. Chem. Soc. **128**, 2816 (2006).
[8] S. R. Mercier, O. V. Boyarkin, A. Kamariotis, M. Guglielmi, I. Tavernelli, M. Cascella, U. Rothlisberger, and T. R. Rizzo, J. Am. Chem. Soc. **128**, 16938 (2006).
[9] J. A. Stearns, S. Mercier, C. Seaiby, M. Guidi, O. Boyarkin, and T. R. Rizzo, J. Am. Chem. Soc. **129**, 11814 (2007).
[10] R. Cohen, B. Brauer, E. Nir, L. Grace, and M. S. de Vries, J. Phys. Chem. A **104**, 6351 (2000).
[11] M. Gerhards and C. Unterberg, Phys. Chem. Chem. Phys. **4**, 1760 (2002).
[12] M. Gerhards, C. Unterberg, and A. Gerlach, Phys. Chem. Chem. Phys. **4**, 5563 (2002).
[13] M. Gerhards, C. Unterberg, A. Gerlach, and A. Jansen, Phys. Chem. Chem. Phys. **6**, 2682 (2004).
[14] H. Fricke, A. Gerlach, and M. Gerhards, Phys. Chem. Chem. Phys. **8**, 1660 (2006).
[15] MACROMODEL, version 9.1, Schrödinger, LLC, New York (2005).
[16] W. D. Cornell, P. Cieplak, C. I. Bayly, I. R. Gould, K. W. Merz, Jr., D. M. Ferguson, D. C. Spellmeyer, T. Fox, J. W. Caldwell, and P. A. Kollman, J. Am. Chem. Soc. **117**, 5179 (1995).
[17] M. J. Frisch, G. W. Trucks, H. B. Schlegel, G. E. Scuseria, M. A. Robb, J. R. Cheeseman, J. J. A. Montgomery, T. Vreven, K. N. Kudin, J. C. Burant, J. M. Millam, S. S. Iyengar, J. Tomasi, V. Barone, B. Mennucci, M. Cossi, G. Scalmani, N. Rega, G. A. Petersson, H. Nakatsuji, M. Hada, M. Ehara, K. Toyota, R. Fukuda, J. Hasegawa, M. Ishida, T. Nakajima, Y. Honda, O. Kitao, H. Nakai, M. Klene, X. Li, J. E. Knox, H. P. Hratchian, J. B. Cross, V. Bakken, C. Adamo, J. Jaramillo, R. Gomperts, R. E. Stratmann, O. Yazyev, A. J. Austin, R. Cammi, C. Pomelli, J. W. Ochterski, P. Y. Ayala, K. Morokuma, G. A. Voth, P. Salvador, J. J. Dannenberg, V. G. Zakrzewski, S. Dapprich, A. D. Daniels, M. C. Strain, O. Farkas, D. K. Malick, A. D. Rabuck, K. Raghavachari, J. B. Foresman, J. V. Ortiz, Q. Cui, A. G. Baboul, S. Clifford, J. Cioslowski, B. B. Stefanov, G. Liu, A. Liashenko, P. Piskorz, I. Komaromi, R. L. Martin, D. J. Fox, T. Keith, M. A. Al-Laham, C. Y. Peng, A. Nanayakkara, M. Challacombe, P. M. W. Gill, B. Johnson, W. Chen, M. W. Wong, C. Gonzalez, and J. A. Pople, GAUSSIAN 03, Revision D.01, Gaussian, Inc., Pittsburgh PA, 2004.
[18] B. Paizs, M. Schnolzer, U. Warnken, S. Suhai, and A. G. Harrison, Phys.

Chem. Chem. Phys. **6**, 2691 (2004).
[19] H. Kang, C. Jouvet, C. Dedonder-Lardeux, S. Martrenchard, G. Gregoire, C. Desfrancois, J. P. Schermann, M. Barat, and J. A. Fayeton, Phys. Chem. Chem. Phys. **7**, 394 (2005).
[20] G. Gregoire, C. Jouvet, C. Dedonder, and A. L. Sobolewski, J. Am. Chem. Soc. **129**, 6223 (2007).
[21] A. Kamariotis, O. V. Boyarkin, S. R. Mercier, R. D. Beck, M. F. Bush, E. R. Williams, and T. R. Rizzo, J. Am. Chem. Soc. **128**, 905 (2006).